

Stack formation during random sequential adsorption of needles onto a square lattice

Mikhail V. Ulyanov,^{1,2} Yuri Yu. Tarasevich,^{3,*} Andrei V. Eserkepov,³ and Irina V. Grigorieva⁴

¹*V. A. Trapeznikov Institute of Control Sciences of RAS, Moscow 117997, Russia*

²*Computational Mathematics and Cybernetics, M. V. Lomonosov Moscow State University, Moscow 119991, Russia*

³*Laboratory of Mathematical Modeling, Astrakhan State University, Astrakhan 414056, Russia*

⁴*Kemerovo State University, Kemerovo 650000, Russia*

(Dated: February 28, 2022)

Using computer simulation, we have studied the random sequential adsorption of stiff linear segments (needles) onto a square lattice. Each such particle occupies k adjacent lattice sites, thence, it is frequently called a k -mer. During deposition, the two mutually perpendicular orientations of the particles are equiprobable, hence, a macroscopically isotropic monolayer is formed. However, this monolayer is locally anisotropic, since the deposited particles tend to form so-called “stacks”, i.e., domains of particles with the same orientation. Using the “excluded area” concept, we have classified lattice sites into several types and examined how the fraction of each type of lattice site varies as the number of deposited particles increases. The behaviors of these quantities have allowed us to identify the following stages of stack formation (i) the emergence of stack seeds; (ii) the filling of stacks; (iii) densification of the stacks.

I. INTRODUCTION

Random sequential adsorption (RSA) is a process during which particles are randomly and irreversibly deposited onto a substrate without overlapping with previously adsorbed particles. RSA is a useful model for many physical, chemical, and biological processes [1, 2]. Both continuous and discrete substrates can be considered. A widely used kind of discrete substrate is the square lattice. One of the simplest particle shapes is the so-called k -mer (rod, stick, needle, stiff linear chain), i.e., a linear “molecule” occupying k adjacent lattice sites. The prohibition of overlapping means a hard-core (excluded volume) interaction between the particles. As particles deposit, first there occurs a percolation phase transition, i.e. the emergence of a cluster that penetrates the whole system. Then, the system reaches a jamming state when any additional deposition of particles is impossible due to the absence of any appropriate empty space to place even one extra particle. Although there are some empty spaces, these holes have inappropriate shapes or sizes to accept a further particle. During the RSA of rods onto a square lattice, the excluded area effect [3] leads to the formation of stacks, i.e., regions filled with particles all of the same orientation. Stack structures have been observed both at percolation [4] and at jamming [5]. Using a local order parameter, the typical size of stacks has been evaluated as $k \times k$ [6]. Thus, although a monolayer produced by RSA is macroscopically isotropic, microscopic regions can exhibit significant anisotropy. Visually, the stacks look like winding areas with dense centers and diffuse edges [7]. It seems, therefore, that a local order parameter cannot provide complete information about the shape and structure of the stacks. An alternative characteristic of the stack structure may be the pair correlation

function [8].

The kinetics of particle deposition has been studied in many works, in particular, analytical expressions for the deposition of disks on the surface [9, 10] and on the lattice [11–14] have been obtained. During RSA, the coverage of the lattice with particles $\Theta(t)$ is known to vary when the adsorption time is large, as

$$\Theta(t) \approx \Theta(\infty) - \exp\left(-\frac{t}{\sigma}\right), \quad (1)$$

where t is the physical time, which takes into account unsuccessful placement attempts, σ is an adjustable parameter, and $\Theta(\infty)$ is the jamming concentration [15–17]. When the substrate is continuous, the coverage depends on time, according to a power law [1].

Due to the exponential dependence of the coverage on time, generating a jamming state on a computer is a very time-consuming task. The jamming state is achievable, generally speaking, only after an infinitely long time. The problem can be solved technically in various ways [18], including by compiling lists of the sites available for particle deposition [1, 7, 19–21]. During the initial stage, straightforward random selection of possible adsorption sites is used. After reaching a certain concentration, such lists of sites available for particle deposition are then created. Next, the new sites for placing particles are selected from these lists. In fact, the lists have to be updated after each successful deposition of a particle. This approach, at a minimum, guarantees the achievement of the jamming state in a finite time. It is clear that the use of lists from the very beginning of the process of particle deposition would not increase the speed of particle placement, but actually lead to significant additional memory costs. Applying lists does ensure that each attempt to place a particle will be successful; however, the formation of the lists requires a significant amount of time, depending on the current fraction of the filling of the lattice. In addition, since some lattice sites may be available for both the vertical and horizontal placement of particles, updating

*Corresponding author: tarasevich@asu.edu.ru

of both lists may be necessary after placing each particle. The question remains: at what concentration does the use of lists become effective?

By means of both computer simulation and analytical treatment using the “excluded area” concept, we have studied the formation of stacks during RSA of rods onto a square lattice. Several stages have been found and classified. This classification provides a clear criterion for when the use of lists of empty sites can ensure more efficient calculation of the deposition of particles.

The rest of the paper is constructed as follows. In Sec. II, the technical details of the simulations are described, all necessary quantities are defined, and some estimates of the finite-size effect are given. Section III presents our principal findings. Section IV summarizes the main results.

II. COMPUTATIONAL MODEL

A square lattice with $L \times L$ sites was used as a substrate. Periodic boundary conditions were applied along both directions of the lattice to reduce the finite-size effect. Linear particles occupying k adjacent lattice sites were randomly and sequentially deposited onto the lattice. To distinguish the two possible orientations of deposited particles, we denoted the particles oriented along the abscissa as k_x -mers, while the particles oriented along the ordinate were k_y -mers. We treated the leftmost site of a k_x -mer and the topmost site of a k_y -mer as the “primary element” (origin) of the particle. The rest of the $k - 1$ sites of the particle were denoted as its body. Both the mutually perpendicular orientations of deposited particles taken as equiprobable. In our simulations, we used $k \in [2; 12]$. As a basis, the linear size of the lattice was chosen as $L = 32k$. However, the finite-size effect has also been tested by variations of the lattice size for a fixed value of k . All results were averaged over 100 independent runs.

We used the reduced (normalized) coverage, i.e., the number of occupied sites, N , divided by the number of occupied sites at jamming, N_j ,

$$x = \frac{N}{N_j}, \quad (2)$$

in such a way that $x \in [0; 1]$.

Each adsorbed particle blocks k lattice sites from further deposition of both k_x - and k_y -mers. Furthermore, some sites in the vicinity of the adsorbed particle are forbidden for the deposition of only one kind of particle (Fig. 1). Figure 1a demonstrates a k_x -mer and a k_y -mer together with their non-overlapping excluded areas. Figure 1b demonstrates a k_x -mer and a k_y -mer when their excluded areas are partially overlapping. Deposited particles are shown using solid fill. Darker cells correspond to the “primary element” of particles, while lighter ones form their bodies. “Primary elements” of any additional

k_x - or k_y -mers can be placed in open cells. Only k_y -mers The “primary elements” of can be placed in cells with vertical hatching. The “primary elements” of only k_x -mers can be placed in cells with horizontal hatching. The “primary elements” of neither k_x - nor k_y -mers can be placed into cross-hatched cells. We classified each of the lattice sites under one of several types:

Type 0 Lattice sites that are forbidden for the deposition of both k_x - and k_y -mers. This type can be additionally divided into two subtypes:

Subtype -0 Occupied sites (filled squares in Fig. 1a). No site of the newly deposited particle can be placed in these sites.

Subtype $+0$ Empty sites that are forbidden for the deposition of the “primary elements” of both k_x - and k_y -mers. However, a body-site of a newly deposited particle may be placed into a site of subtype $+0$. These sites are shown in Fig. 1b as cross-hatched squares.

Type 1 Empty sites that allow deposition of the “primary elements” of the either k_x - or k_y -mers. These sites are shown in Fig. 1 as horizontally, or vertically hatched squares, respectively.

Type 2 Empty sites that can allow the deposition of the “primary elements” of both k_x - and k_y -mers. These sites are shown in Fig. 1 as open squares.

Sites of types 0 and 1 belong to the excluded area.

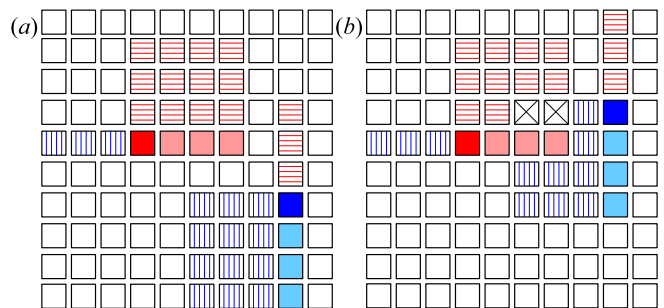


FIG. 1: Example of a k_x -mer and a k_y -mer ($k = 4$) with (a) non-overlapping excluded areas and (b) partially overlapping excluded areas.

The fractions of lattice sites belonging to one of these types are denoted as $f_{-0}(x)$, $f_{+0}(x)$, $f_1(x)$, and $f_2(x)$, respectively. Naturally, $f_{-0}(x) + f_{+0}(x) + f_1(x) + f_2(x) = 1$, hence, only three of the four functions are independent. By definition, $f_{-0}(x)$ is a linear function. It is therefore uninformative, and is not discussed further.

Figure 2 presents an example of the functions $f_{+0}(x)$, $f_1(x)$, and $f_2(x)$ for one particular case ($k = 8$, $L = 256$). $f_2(x)$ is a monotonically decreasing function, while each of the functions $f_{+0}(x)$ and $f_1(x)$ has one maximum and one inflection point. The coordinates of the maxima

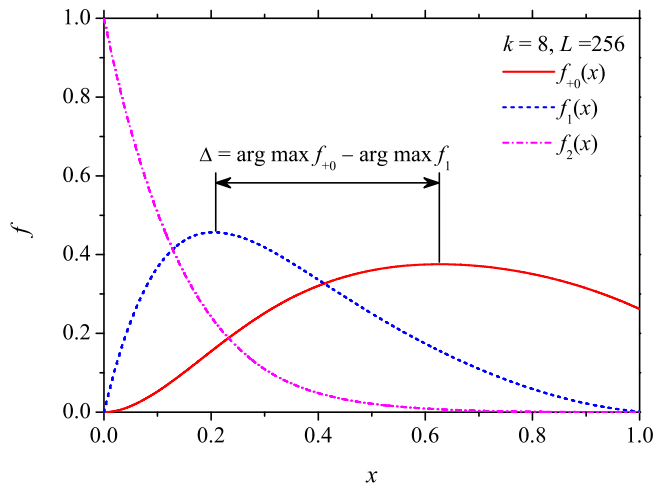


FIG. 2: Example of the functions $f_{+0}(x)$, $f_1(x)$, and $f_2(x)$ for $k = 8$, $L = 256$.

look promising for characterizing the kinetics of stack formation.

Figure 3 presents the functions $f_{+0}(x)$ and $f_1(x)$ for a fixed $k = 8$ and different lattice sizes ($L = 64, 256, 1024$). Figure 3 suggests that the finite-size effect is significant only in the vicinity of the jammed state ($x = 1$). In any case, the curves for $L = 32k$ and $L = 128k$ are hardly distinguishable. Since stack formation is a continuous process, i.e., there is no jump between any two stages, the exact location of the maxima is not so important. This is the reason for the use of $L = 32k$ in our main evaluations.

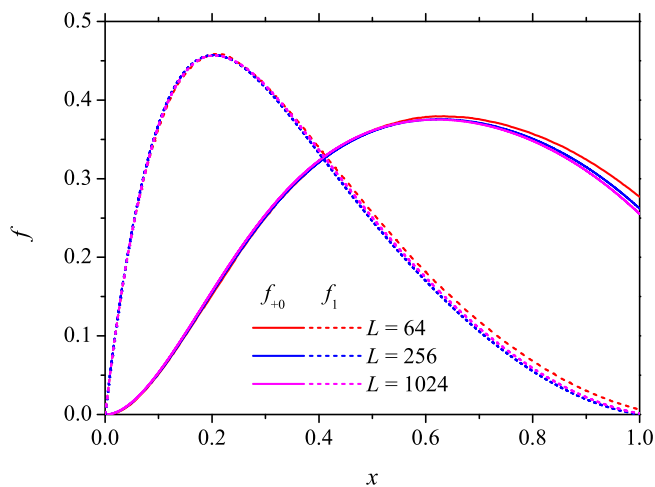


FIG. 3: Example of the finite-size effect: functions $f_{+0}(x)$ and $f_1(x)$ for $k = 8$, $L = 64, 256, 1024$.

III. RESULTS AND DISCUSSION

For $k \in [2; 12]$, the abscissae of the critical points of the functions $f_1(x)$ and $f_{+0}(x)$ decrease as the value of k increases (Fig. 4). However, this behavior may differ for larger values of k .

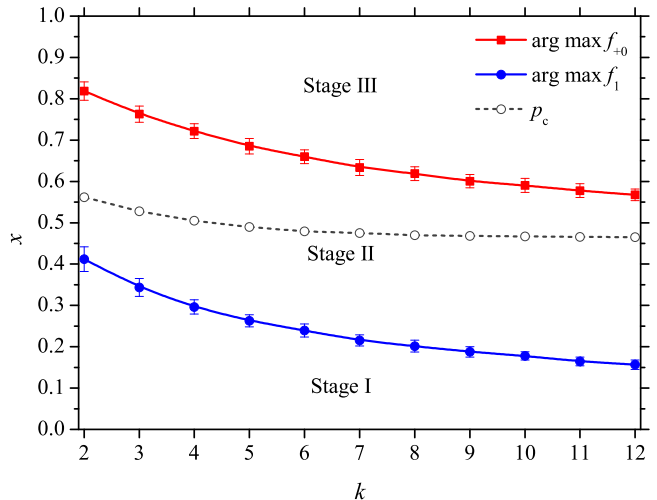


FIG. 4: Dependencies of $\arg \max f_{+0}$, $\arg \max f_1$, and the percolation threshold, p_c , on the particle size, k . The lines between the markers are drawn simply for convenience.

The critical points of the functions $f_1(x)$ and $f_{+0}(x)$ as well as direct observation of the particle deposition [23] suggest the following stages of stack formation. Naturally, the boundaries of the stages are approximate (Fig. 4).

Stage I: Emergence of stack seeds. During the initial stage of particle deposition ($x \in [0; \arg \max f_1(x)]$), particles stake out the future stacks. The number of empty sites of type 2 decreases, while the number of empty sites of type 1 increases. Since a significant fraction of the empty sites can accept deposited particles of only one orientation, these domains can be treated as the progenitors of future stacks (Figs. 6 and 5a).

Stage II: Filling of stacks. As the number of deposited particles increases ($x \in [\arg \max f_1(x); \arg \max f_{+0}(x)]$), the number of sites of type 1 decreases due to overlapping of the excluded areas produced by the deposited particles of mutually perpendicular orientations (Figs. 7 and 5b).

Stage III: Densification of stacks. At this stage ($x \in [\arg \max f_{+0}(x); 1]$), almost all newly deposited particles fall only into the already formed stacks. A feature of this stage is the reduction in the number of sites of type +0 due to their overlapping by newly deposited particles. At this stage, the number of sites of type 2 is already negligible. A reduction in the number of sites of type 1 occurs since the newly deposited particles overlap sites of types 1 and +0. Almost all newly deposited particles are placed into already formed and limited stack structures. This densification of the stacks little changes their

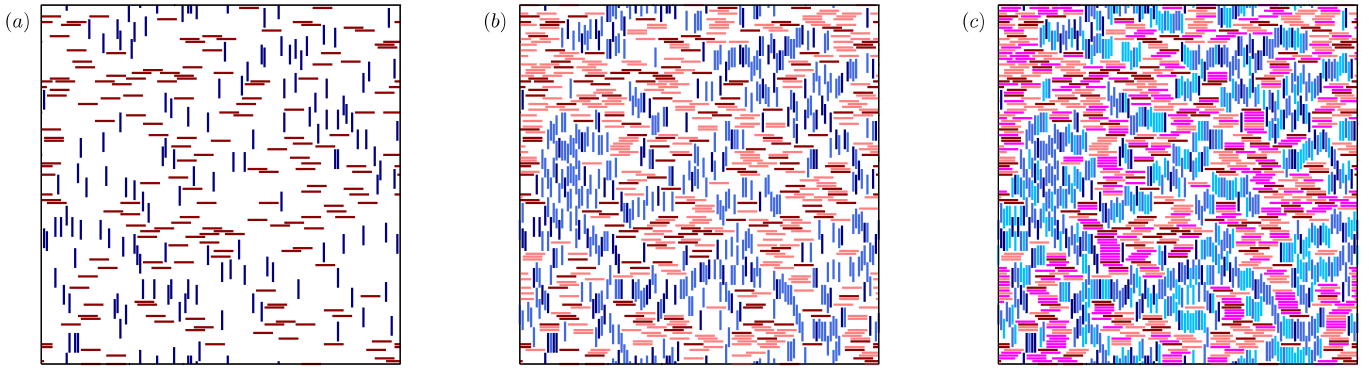


FIG. 5: Example of the sequence of formation of the stack structure for one particular lattice ($k = 8$, $L = 16k$). The patterns at the end of each stage are shown. (a) I, (b) II, and (c) III. Particles deposited during each particular stage are shown in different shades.

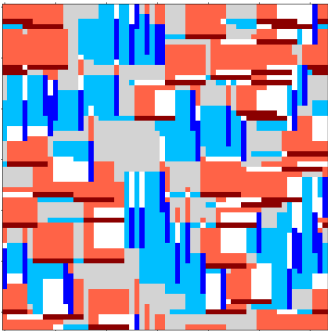


FIG. 6: Example of a system under consideration, at the end of stage I. Both deposited particles and different types of sites are shown, $k = 8$, $L = 8k$.

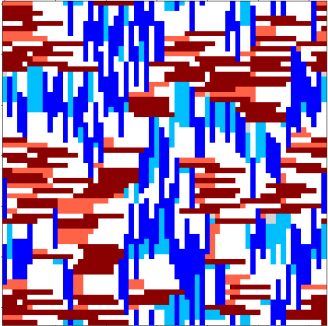


FIG. 7: Example of a system under consideration at the end of stage II. Both deposited particles and different types of sites are shown, $k = 8$, $L = 8k$.

formed structure, since almost all the newly deposited particles are placed inside stacks between, and aligned with, previously placed particles (Fig. 5c).

For the values of k under consideration, the width of stage II seems to be a constant within the precision of our evaluations

$$\Delta = \arg \max f_{+0} - \arg \max f_1 \approx 0.42 \pm 0.01.$$

With increasing value of k , the width of stage I decreases

while that of stage III increases.

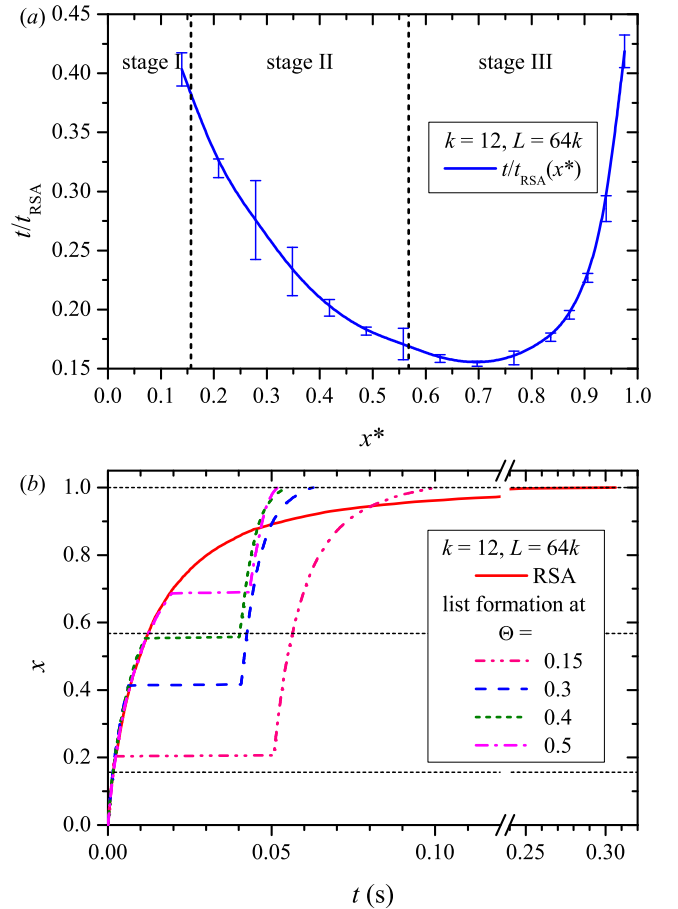


FIG. 8: (a) Example of the dependence of the reduced time required to achieve jamming, t/t_{RSA} , on the concentration, x^* , at which the formation of lists of site available for particle deposition begins. $k = 12$, $L = 64k$. (b) Example of the reduced lattice coverage, x , vs time, t . Horizontal parts of the curves correspond to the formation of lists.

The start of stage III appears to present an appropriate

moment at which to build up the lists of available sites for the deposition of k_x - and k_y -mers (Fig. 8a). These lists will be almost non-overlapping since the fraction of particles of type 2 is negligible ($f_2(x) \approx 0$). Figure 8b presents the dependency of the reduced lattice coverage, x , on the CPU time, t , for different cases, viz., (i) straightforward realization of the RSA (random choice of the lattice site to deposit the new particle) and (ii) random choice from the lists of the sites available for the deposition k_x - and k_y -mers; in the latter case the lists were compiled when three different lattice coverages had been reached.

IV. CONCLUSION

Using computer simulation, we have studied an isotropic random sequential adsorption of stiff linear segments (needles) onto a square lattice with periodic boundary conditions along both directions. Due to the excluded area effect, deposited particles form so-called

stacks, i.e., domains of particles of the same orientation. Using the excluded area concept, we have classified lattice sites into several types. We have examined how the fraction of each type of lattice site varies with the number of deposited particles. The behaviors of these quantities provide for a classification of the stages of stack formation: (i) the emergence of stack seeds; (ii) the filling of stacks; (iii) densification of the stacks. When lists of empty sites are to be used in a computer program to accelerate the achievement of the jammed state, the start of stage III appears to be the appropriate moment to build up such lists. Since our study is restricted only to short particles, an additional study is needed for larger values of k ($k > 12$).

Acknowledgments

We acknowledge funding from the Russian Foundation for Basic Research, Project No. 18-07-00343.

-
- [1] J. W. Evans, Random and cooperative sequential adsorption, *Rev. Mod. Phys.* **65**, 1281 (1993).
 - [2] Z. Adamczyk, Modeling adsorption of colloids and proteins, *Curr. Opin. Colloid Interface Sci.* **17**, 173 (2012).
 - [3] L. Onsager, The effects of shape on the interaction of colloidal particles, *Ann. N. Y. Acad. Sci.* **51**, 627 (1949).
 - [4] Y. Leroyer and E. Pommiers, Monte Carlo analysis of percolation of line segments on a square lattice, *Phys. Rev. B* **50**, 2795 (1994).
 - [5] N. Vandewalle, S. Galam, and M. Kramer, A new universality for random sequential deposition of needles, *Eur. Phys. J. B* **14**, 407 (2000).
 - [6] Y. Y. Tarasevich, A. V. Eserkepov, V. V. Chirkova, and V. A. Goltseva, Monte Carlo simulation of entropy-driven pattern formation in a two-dimensional system of rectangular particles, *J. Phys. Conf. Ser.* **1163**, 012007 (2019).
 - [7] M. G. Slutskii, L. Y. Barash, and Y. Y. Tarasevich, Percolation and jamming of random sequential adsorption samples of large linear k -mers on a square lattice, *Phys. Rev. E* **98**, 062130 (2018).
 - [8] R. C. Hart and F. D. A. Aarão Reis, Random sequential adsorption of polydisperse mixtures on lattices, *Phys. Rev. E* **94**, 022802 (2016).
 - [9] J. W. Evans, Comment on “Kinetics of random sequential adsorption”, *Phys. Rev. Lett.* **62**, 2642 (1989).
 - [10] P. Schaaf, A. Johner, and J. Talbot, Asymptotic behavior of particle deposition, *Phys. Rev. Lett.* **66**, 1603 (1991).
 - [11] D. K. Hoffman, On the nonequilibrium distribution of adatoms resulting from dissociative adsorption of a diatomic gas, *J. Chem. Phys.* **65**, 95 (1976).
 - [12] J. W. Evans, Irreversible random and cooperative process on lattices: Direct determination of density expansions, *Physica A* **123**, 297 (1984).
 - [13] J. W. Evans, Nonequilibrium percolative $c(2 \times 2)$ ordering: Oxygen on Pd(100), *J. Chem. Phys.* **87**, 3038 (1987).
 - [14] A. Baram and D. Kutasov, On the dynamics of random sequential absorption, *J. Phys. A: Math. Gen.* **22**, L251 (1989).
 - [15] V. Privman, J.-S. Wang, and P. Nielaba, Continuum limit in random sequential adsorption, *Phys. Rev. B* **43**, 3366 (1991).
 - [16] V. Cornette, D. Linares, A. J. Ramirez-Pastor, and F. Nieto, Random sequential adsorption of polyatomic species, *J. Phys. A: Math. Theor.* **40**, 11765 (2007).
 - [17] L. Budinski-Petković, S. B. Vrhovac, and I. Lončarević, Random sequential adsorption of polydisperse mixtures on discrete substrates, *Phys. Rev. E* **78**, 061603 (2008).
 - [18] M. Cieřla, Effective modelling of adsorption monolayers built of complex molecules, *J. Comput. Phys.* **401**, 108999 (2020).
 - [19] R. S. Nord, Irreversible random sequential filling of lattices by Monte Carlo simulation, *J. Stat. Comput. Simul.* **39**, 231 (1991).
 - [20] B. J. Brosilow, R. M. Ziff, and R. D. Vigil, Random sequential adsorption of parallel squares, *Phys. Rev. A* **43**, 631 (1991).
 - [21] C. Fusco, P. Gallo, A. Petri, and M. Rovere, Random sequential adsorption and diffusion of dimers and k -mers on a square lattice, *J. Chem. Phys.* **114**, 7563 (2001).
 - [22] See Supplemental Material at [URL will be inserted by publisher] for an animation of the temporal evolution of stacks for $k = 8$, $L = 16k$.
 - [23] See Supplemental Material at [URL will be inserted by publisher] for an animation of the temporal evolution of stacks for $k = 8$, $L = 16k$.